

# Microwave-Induced Effects on Superconductors\*

E. D. Dahlberg<sup>†</sup> and R. L. Orbach

Physics Department, University of California at Los Angeles, Los Angeles, California

and Ivan Schuller

Physics Department, University of California at Los Angeles, Los Angeles, California  
and Solid State Science Division, Argonne National Laboratory, Argonne, Illinois

(Received January 22, 1979)

*We have studied the effects of microwave radiation on superconducting tunnel junctions and on the critical currents of superconducting strips at 2.0 and 10.0 GHz. In the tunnel junctions both quantum mechanical and classical effects (photon-induced tunneling and classical rectification, respectively), were observed, but not gap enhancement. The application of microwave radiation on long, superconducting, thin-film bridges was found to increase their critical current. The microwave magnetic field was found to couple more efficiently to the superconductor. The increase in the critical current was found to be proportional to the square root of the incident power.*

## 1. INTRODUCTION

Recently there has been renewed interest concerning the interaction of microwave radiation with superconductivity. This was stimulated by the experiments of Klapwijk and Mooij<sup>1</sup> on long, thin superconducting films. They found that when the photon energy is less than the superconducting energy gap the critical currents of these films increases markedly. The increase in the critical currents was found to be dependent on both the frequency and power of the incident radiation. It was suggested that a possible explanation of their results lay with the theory of Eliashberg.<sup>2</sup> The quasiparticles absorb the microwave energy and thereby move to higher energy states (since the microwave frequency is smaller than the energy gap, there is no pair breaking). Since the superconducting energy gap is more dependent upon the availability of the *low*-lying energy levels, the gap will be enhanced. This hypothesis has been tested in a direct fashion by

\*Work supported in part by grants NSF DMR # 76-82347 and ONR NOO14-75-C-0245 P4.

<sup>†</sup>Present address: Physics Department, University of Minnesota, Minneapolis, Minnesota.

Kommers and Clarke<sup>3</sup> on Al-I-Al tunnel junctions. They observed an increase in the energy gap of both Al films while the films were being irradiated with microwaves. This experiment is the basis for the belief that one can in fact increase the energy gap of superconductors by irradiation with microwaves, where the photon energy is less than the energy gap. Motivated by these results, we have undertaken detailed experiments to simultaneously study the effects of microwaves on long strips as well as tunnel junctions.

In the next section we describe earlier experiments and theories. In Section 3 we present our experimental results and their interpretation and in Section 4 our conclusions are presented.

## 2. EARLY EXPERIMENTS AND THEORIES

Dayem and Martin<sup>4</sup> studied the effects of 25–63-GHz microwave radiation on Al-I-Pb, Al-I-In, and Al-I-Sn tunnel junctions. In addition to the usual structure at  $\Delta_1 \pm \Delta_2$  on the  $I$ - $V$  characteristic, they also found steps at

$$|eV| = \Delta_1 \pm \Delta_2 \pm nh\nu \quad (1)$$

where  $\Delta_1$  and  $\Delta_2$  are the temperature-dependent values of the energy gap parameters of the Al and either Pb, In, or Sn;  $\nu$  is the microwave radiation frequency; and  $n$  is an integer.

This was interpreted as the quantum absorption or emission of an integer number of incident photons allowing a particle to tunnel across the oxide layer. Dayem and Martin did not report on observation of gap enhancement. This is consistent with the idea that the microwave frequency has to be larger than  $1/\tau_e$  (much shorter for Sn, In, and Pb than for Al<sup>5</sup>). Tien and Gordon<sup>6</sup> treated this situation theoretically by assuming that the effect of the microwaves is to add an oscillatory electric field across the junction. This has the effect of changing the electron energies adiabatically. They found the modified tunneling current to be given by

$$I(V_{dc}) = \sum_{n=-\infty}^{\infty} J_n^2(\alpha) I_0(V_{dc} + n\hbar\omega/e), \quad \alpha = eV_{rf}/\hbar\omega \quad (2)$$

where  $V_{dc}$  is the dc applied voltage,  $J_n$  is the  $n^{\text{th}}$ -order Bessel function of the first kind,  $V_{rf}$  is the microwave-induced rf voltage,  $n$  is an integer,  $\omega$  is the microwave frequency, and  $I_0(V)$  is the tunneling current at the voltage  $V$  in the absence of microwaves.

It was later pointed out by Hamilton and Shapiro<sup>7</sup> that due to the finite width of the BCS singularities in the density of states there are two regimes:

high frequency ( $h\nu/e >$  microwave step width) and low frequency ( $h\nu/e <$  microwave step width). In the *high-frequency regime* the Tien and Gordon result is valid if there is no variation of the microwave field across the dimensions of the junctions.\* If the microwave wavelength in the junction is comparable to the junction dimension, the Bessel function dependence of the steps is modified. In this situation the microwave steps show a peak and then gradually decrease to a roughly constant value as a function of microwave voltage. In the *low-frequency regime* the microwave steps are not observable (only a gradual change on the  $I$ - $V$  characteristic) and the Tien-Gordon formula reduces to the classical rf detection formula,

$$I_{dc}(V_{dc}) = \pi^{-1} \int_{-\pi/2}^{\pi/2} I_0(V_{dc} + V_{rf} \sin \theta) d\theta \quad (3)$$

Using a computer simulation of Eq. (4), Hamilton and Shapiro showed that the sharp structure in the tunneling characteristic becomes smeared out into two structures, one at  $V_{dc} - V_{rf}$  and one at  $V_{dc} + V_{rf}$ . The crossover point from the quantum mechanical picture to the classical picture occurs when the energy width of the structure in the tunneling characteristic goes from less than a single photon energy to more than a single photon energy. Thus far the microwave source has been treated as a voltage generator. This assumes the junction resistance is large. The reverse of this (junction resistance less than impedance of microwave source) has been investigated experimentally by Tulin<sup>9</sup> for the classical case. His main result is that the smearing of a structure is observed only at  $V_{dc} + V_{rf}$ , not at  $V_{dc} - V_{rf}$ . He was able to computer fit his data by varying the ratio of the junction resistance to the microwave source.

The first experimental work on the effects of microwave radiation on weak links was done by Anderson and Dayem<sup>10</sup> and later in more detail by Dayem and Wiegand.<sup>11</sup> They observed an increase in the critical current of indium weak links ( $2 \times 0.1 \mu\text{m}$ ) during exposure to microwave radiation.

Hunt and Mercereau<sup>12</sup> argued that if the two larger portions of a superconducting film, i.e., the portions separated by the constriction or the weak link, are weakly coupled, the quantum mechanical phases may be different, generating an extra degree of freedom and thus a lower energy. If this energy is greater than the difference in energy of the link in the superconducting and normal states, then the constriction would remain normal below its expected  $T_c$  (transition temperature of the banks). The energy lost by forcing the constriction to remain normal will be proportional to its volume, but the length must be such that an electron traveling from one side to the other will lose its phase memory (greater than a coherence

\*It was shown by Swihart<sup>8</sup> that the microwave wavelength can be appreciably different inside the junction compared to the wavelength inside the waveguide in the absence of the junction.

length). If the temperature is lowered until the constriction becomes superconducting, the critical value for the current density would be less than one would have expected for the bulk material. Hunt and Mercereau proposed that the microwave radiation would couple the phases of the two superconducting regions and therefore lose some of this extra degree of freedom for a given radiation frequency and power level. This would manifest itself by increasing  $T_c$  to its bulk value and increasing the critical current accordingly.

A similar theory was advanced by Lindelof.<sup>13</sup> He considered the situation in which the pair potential  $\Delta$  in a given region of a superconducting film is lower than that in the remainder of the film. Then the density of Cooper pairs in this region  $n_s$  will be lowered ( $n_s \propto \Delta^{1/2}$ ). With this assumption, Lindelof argues that the measured pair potential in this region can now be increased in the following way. A high-frequency current in a superconductor will consist of both Cooper pairs and quasiparticles (except at  $T = 0$  K, where there are no quasiparticles). This is because the inertia or self-inductance of the pairs will not allow an infinitely fast response to an external electric field. Therefore, before the electric field inside the superconductors is reduced to zero the quasiparticles will have been accelerated, leading to a net quasiparticle velocity. The proportioning of the current between the pairs and quasiparticles is dependent on how many of each are present. Therefore in the region where the pair potential is small, one expects the current leaving this region to have a larger proportion of quasiparticles than the current coming into this region (charge neutrality must be maintained). This creates a momentary situation where  $n_s$  is larger in the small pair potential region than in equilibrium, leading to a larger  $\Delta$ . For this to work, however, the pairs must be injected into this region faster than it takes to restore equilibrium. Thus, if the microwave radiation is at a higher frequency, than  $1/\tau$ , the temperature-dependent quasiparticle recombination frequency than the average value of  $\Delta$  is increased. The measured critical current is determined by that of the region with the smallest number of pairs. The net effect of the microwave, therefore, is to increase the critical current of the film.

The self-consistent equation for the energy gap parameter  $\Delta$  from the BCS theory of superconductivity is given by

$$\Delta = N_0 V \int_{\Delta}^{\hbar\omega_D} \Delta [1 - 2f(\varepsilon)] / (\varepsilon^2 - \Delta^2)^{1/2} d\varepsilon \quad (4)$$

where  $N_0$  is the density of states at the Fermi surface in the normal state,  $V$  is the attractive interaction parameter,  $\varepsilon$  is the energy of a quasiparticle measured with respect to the Fermi surface,  $\omega_D$  is the Debye frequency, and

$f(\epsilon)$  is the distribution function of the quasiparticles. Equation (4) shows that the value of  $\Delta$  is related to the distribution of quasiparticles through  $f(\epsilon)$ . Eliashberg<sup>2</sup> suggested that if the quasiparticle distribution can be altered by raising quasiparticles from low-lying energy states to higher ones, then  $\Delta$  will increase. This can be accomplished with electromagnetic radiation (i.e., microwaves) if the energy of a single photon is less than that necessary to break apart a Cooper pair ( $h\nu/e < 2\Delta$ ) but with a frequency greater than  $1/\tau_0$ , the characteristic "in-branch" relaxation time of the quasiparticles to decay back to the equilibrium. By solving self-consistently a Boltzman-like kinetic equation for the quasiparticles and phonons, Chang and Scalapino<sup>14</sup> have shown that (mainly due to effects associated with the quasiparticle redistribution) the microwave irradiation will produce gap enhancement.

We should point out that all the above theories require the cross-sectional dimension of the films to be small compared to the penetration depth to ensure homogenous field strength in the films.

### 3. EXPERIMENTAL RESULTS

Approximately 50 tunnel junctions or strips were measured, with essentially the same results. For simplicity we only present representative data from a few samples.

The measurements of the critical currents of the Al strips and the current-voltage characteristics of the tunnel junctions were performed using a constant-current source. The current passing through the sample was measured by monitoring the voltage across a resistor in series with the sample. Both the strips and the tunnel junctions were connected to make usual four-probe measurements. The critical currents of the strips were measured directly using an oscilloscope, while the characteristics of the tunnel junctions was measured using a standard tunneling bridge.

The samples were prepared on fused quartz, sapphire, or BaF substrates. Care was taken to avoid heating the substrates by the microwaves. The samples were prepared in various pressures ranging from  $1 \times 10^{-6}$  to  $5 \times 10^{-5}$  Torr to determine the effect of granularity. Some samples were prepared on substrates heated to  $\sim 200^\circ\text{C}$  in order to increase grain size.

The temperature was measured and controlled to better than 1 mK with two shielded germanium resistors. Extreme care was taken to avoid altering the temperature reading in an artificial manner because of the presence of microwave radiation.

For the irradiation of the strips and tunnel junctions with 10-GHz microwave radiation, a 300-mW klystron, an adjustable attenuator, an adjustable short, and various lengths of waveguide were used. The samples were mounted with rubber cement (in contact with the substrate, not the

metallic films) in a section of waveguide, just before the adjustable short, and parallel to the larger dimension wall of the waveguide. The plane of the films was thereby parallel to the microwave magnetic field  $h_{rf}$  (electric field  $e_{rf}$  perpendicular). The adjustable short allowed the position of the rf field maxima and minima, relative to the samples, to be altered during the experiments. Only the  $TE_{10}$  mode of the propagation was considered for the determination of field configuration. The leads attached to the samples were shielded with ferrite beads at the point of exit from the waveguide (two holes about 1.5 cm apart in wider plane of guide) to prevent leakage of radiation.

The low-frequency (2.0 GHz, 100 mW) radiation was applied to the samples with a stripline cavity designed for low-frequency ESR measurements.<sup>15</sup> In this case the samples were mounted either at the maximum  $h_{rf}$  or maximum  $e_{rf}$  positions with rubber cement. The leads attached to the sample exited the cavity through the bottom when the  $h_{rf}$  maximum configuration was used or through a slot (1 mm  $\times$  1 cm) cut in the ground plane over the sample when the  $e_{rf}$  configuration was employed. We stress the point that in this fashion the microwave field configuration at the sample was known precisely.

Figure 1 shows the conductance vs. voltage for an Al/Al (1000 Å/1000 Å) tunnel junction prepared on a fused quartz substrate at a

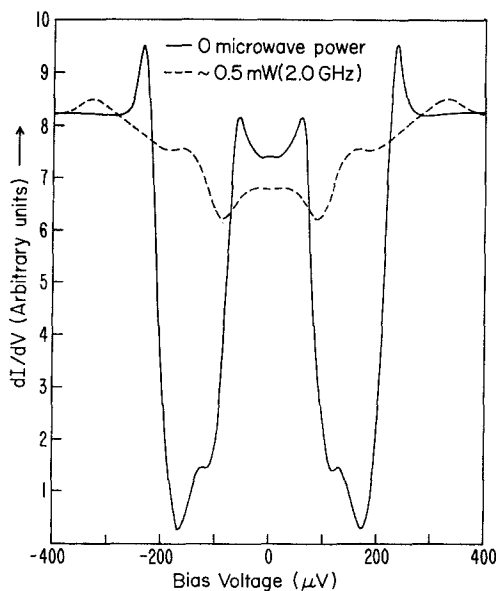


Fig. 1. "Granular" Al/Al (1000 Å/1000 Å) tunnel junction characteristic with and without microwave radiation at  $T = 1.229$  K.

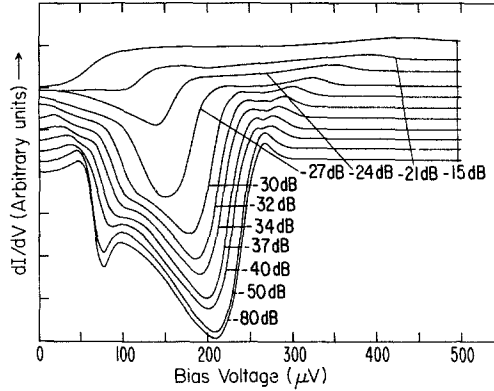


Fig. 2. Evolution of classical rectification effects on "granular" Al/Al tunnel junction at  $T = 1.272$  K as a function of applied 2-GHz microwave power. The curves have been displaced vertically to aid the viewer.

rate of  $10 \text{ \AA}/\text{sec}$  at a pressure of  $\sim 5 \times 10^{-5}$  Torr. The transition temperatures determined from extrapolating the energy gap vs. temperature curves were  $T_{c1} \approx 1.45$  K and  $T_{c2} \approx 1.32$  K. This junction was prepared in order to increase the step width<sup>16</sup> so as to be in the low-frequency regime ( $h\nu/e \sim 8 \text{ } \mu\text{V} < \text{step width}$ ) as explained in Section 2.

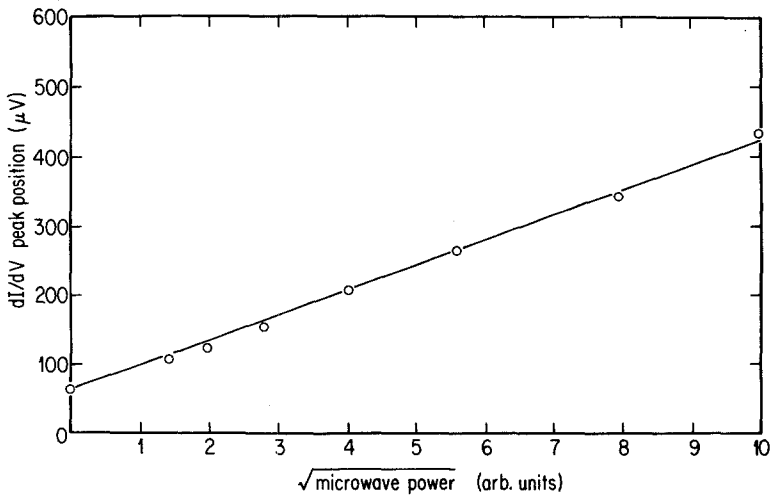


Fig. 3. Position of microwave-radiation-induced peak in tunneling characteristic as a function of the square root of the applied microwave power.

The first peak ( $\sim 60 \mu\text{V}$ ) in the inverse resistance corresponds to the bias voltage being equal to the difference between the energy gaps of the two superconductors ( $\Delta_1 - \Delta_2$ ), while the second peak ( $\sim 235 \mu\text{V}$ ) corresponds to the bias voltage equal to their sum ( $\Delta_1 + \Delta_2$ ). The second curve plotted on the figure exhibits the effect of 0.5 mW of microwave power at 1.98 GHz. Notice the absence of microwave-induced steps and the fact that the point corresponding to  $\Delta_1 + \Delta_2$  has “split” into two peaks ( $\sim 160$  and  $330 \mu\text{V}$ ) symmetric about  $\Delta_1 + \Delta_2$  in the absence of the microwaves.

This splitting is interpreted as due to the classical theory of rectification, where the single photon energy is less than the structure in the tunneling characteristic. The photon energy in this case is about  $8 \mu\text{V}$  ( $h\nu/e$ ), requiring the distribution of values of  $\Delta_1 + \Delta_2$  to be equal to or greater than this value. This junction was made without masking the film edges, so that this energy gap variation is certainly not unreasonable (due to granularity and edge effect).<sup>16</sup> Figure 2 shows the evolution of this structure (and also the  $\Delta_1 + \Delta_2$  splitting more clearly) as a function of the microwave power.

Figure 3 displays the position of the highest voltage peak (measured on a different junction) as a function of microwave voltage (square root of microwave power). Notice that the position of the peak is linearly proportional to the microwave voltage across the junction, and at zero applied microwave voltage the position is that of  $\Delta_1 + \Delta_2$ , as expected. As a second check of this effect, we also have simulated the microwaves by applying an alternating voltage at 40 kHz to the terminal of the tunnel junction and these

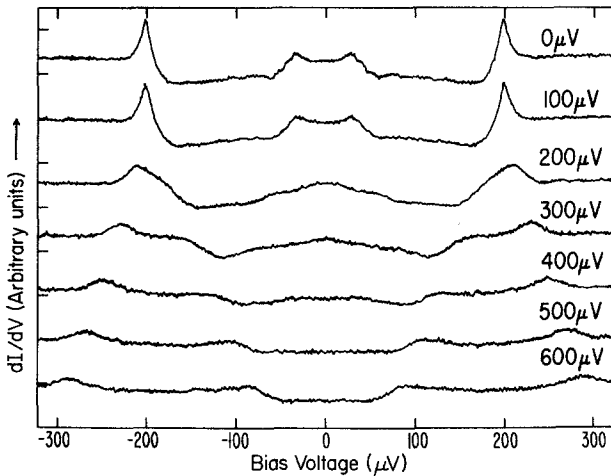


Fig. 4. Tunneling characteristics of tunnel junction exhibiting classical rectification at 40 kHz.



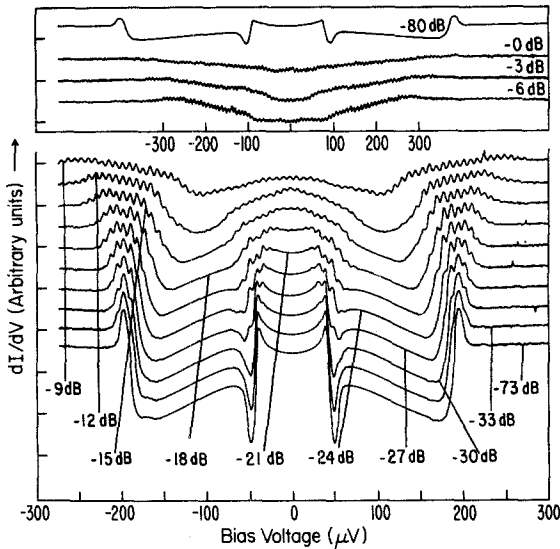


Fig. 5. Microwave-power-dependent evolution of photon-induced tunneling with 2-GHz radiation for a "clean" Al/Al (1000 Å/1000 Å) junction. The upper four curves are with different  $X$  and  $Y$  sensitivities to show all the photon-induced steps.

results are shown in Fig. 4. The similarities in Figs. 4 and 2 indicate that the classical rectification model correctly explains Figs. 1–3.

By masking the edges of the junctions such that tunneling occurs only in the bulk portion of the films and by evaporating at low pressures ( $\sim 10^{-6}$  Torr), the distribution in the values of  $\Delta_1$  and  $\Delta_2$  could be made less than a single photon energy. In this case, quantum effects or photon-induced tunneling was observed. Typical results are shown in Fig. 5. In the upper four curves, the  $x$  sensitivity (or bias voltage scale) has been decreased in order to observe all the photon steps at this power level. The uppermost curve of these four is measured in the absence of microwaves. Thus far, the data presented have been for low-frequency microwaves ( $\sim 2$  GHz). Figure 6 shows photon-induced tunneling due to 9.34-GHz radiation ( $h\nu/e \approx 39 \mu\text{V}$ ). Again the effect of the microwaves is similar to that at 2 GHz, except that now the step separation is the one corresponding to 10 GHz. One important fact to notice is that in the quantum case, the effect of increasing the radiation is to produce more and more microwave steps, but surprisingly enough the gap structure  $\Delta_1 \pm \Delta_2$  seems to remain at the same voltage. For simplicity we have presented only data taken at the lowest

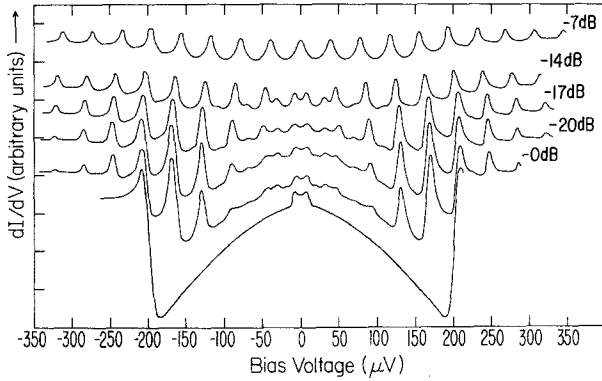


Fig. 6. Microwave-power-dependent evolution of photon-induced tunneling with 9.34-GHz radiation at  $T = 1.245$ .

temperatures. Data taken up to a reduced temperature of 0.995 show the same qualitative behavior.

In summary, we have observed both quantum and classical effects on tunnel junctions, but not gap enhancement. We should point out that for classical rectification the structure at  $\Delta_1 \pm \Delta_2$  moves in a fashion that resembles gap enhancement.

We have also studied the behavior of long (1–2 mm), 100- $\mu\text{m}$ -wide, superconducting bridges under microwave irradiation. Figure 7 exhibits the critical current enhancement of an Al (1000 Å) bridge on a sapphire

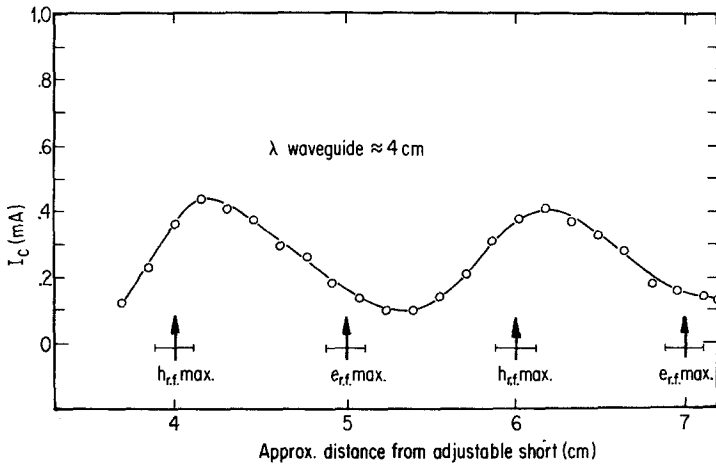


Fig. 7. Field configuration sensitivity of enhanced critical current at fixed microwave power for an Al (1000 Å) film.

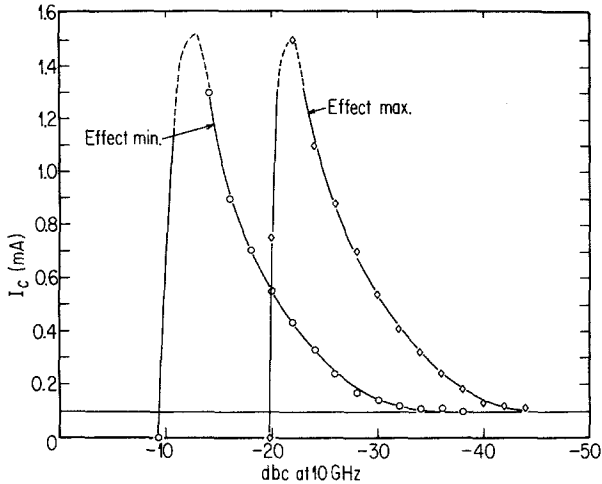


Fig. 8. Dependence of critical current enhancement on applied microwave power for applied  $h_{rf}$  and  $e_{rf}$ .

substrate as a function of field orientation. The field configuration shown in the graph is calculated without the sample in the waveguide.

The field was perpendicular to the surface of the film in the  $e_{rf}$  position and parallel in the  $h_{rf}$  configuration. Also, the films were mounted in the waveguide with two different orientations. In one, the film substrate was mounted flat against one wall of the waveguide with the length of the film parallel to the wider dimension of the waveguide cross section (this geometry will be denoted by G1). The leads in this geometry (four for critical current measurements) exited the waveguide at the ends of the film. Thus, in the  $h_{rf}$  maximum geometry the length of the film was parallel to the  $h$  field, and the film and leads cut a minimum amount of flux lines. For the other geometry, the sample was mounted parallel to the length of the waveguide on a Teflon block about 0.5 cm high. The leads exited the wavelength through the wall (same as in G1) directly below the ends of the film (we denote this geometry by G2). In this geometry, when the  $h_{rf}$  is a maximum, and the film and attached leads are in a plane perpendicular to the field and act like a loop cutting a maximum number of flux lines. The  $e_{rf}$  for both geometries is perpendicular to the plane of the film, and parallel to the leads. The intensity of  $e_{rf}$  in the latter geometry will vary along the length of the film (film length 1 cm and wavelength 4 cm at 10 GHz in the X-band waveguide). For the G1 configuration shown in Fig. 7 the  $h_{rf}$  increases the critical current more effectively than for the configuration G2.

Figure 8 exhibits the critical current as a function of applied microwave power for both  $e_{rf}$  and  $h_{rf}$  field maxima configurations. The figure shows that

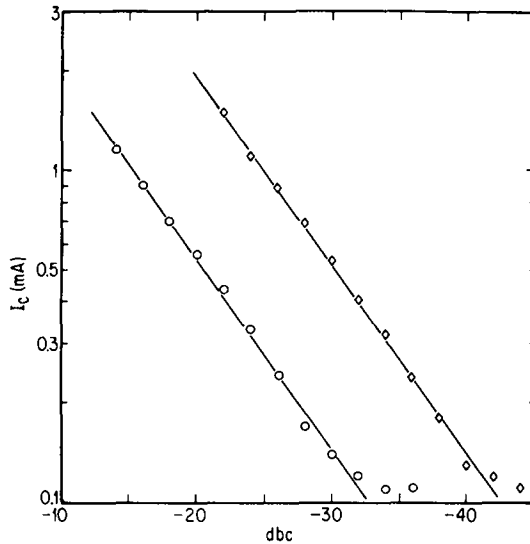


Fig. 9. Log of enhanced critical current vs. log microwave power for applied  $h_{rf}$  and  $e_{rf}$ .

both fields can increase the critical current to roughly the same maximum value before driving the film normal, but the power required for each case is different. Figure 9 is a plot of the log of the critical current vs. the log of the applied power for the data in Fig. 8. The slope of both sets of data shown in this figure is one-half, indicating the enhancement of the critical current is proportional to the square root of the power. The same results were obtained for the G2 geometry in general, but the power necessary for enhancement was less for  $h_{rf}$  maximum than for G1, while the necessary power for enhancement was greater for the G2  $e_{rf}$  when compared to G1. These results are summarized in Table I. These data were accumulated at  $T = 1.257$  K, where the corresponding supercurrent without microwaves

TABLE I

Microwave Power Necessary for Maximum Enhancement of Critical Current for Various Geometries

Field maxima and geometry	Applied microwave power for maximum enhancement of $I_c$ , dBc
G1 $h_{rf}$	-22
G1 $e_{rf}$	-14
G2 $h_{rf}$	-30
G2 $e_{rf}$	-7

was  $1 \times 10^{-6}$  A (first observation of supercurrent occurred at  $T = 1.27$  K). These data were from the same film measured three days apart, with the measured resistivity ratios ( $R_{T=\text{room}}/R_{T=4.2}$ ) showing no aging effects.

Since the critical current enhancement was previously interpreted as gap enhancement, a tunnel junction was manufactured with leads attached so that the critical current of the films could be measured. The critical currents were then measured as the temperature was adjusted until the microwaves produced a maximum enhancement (of  $\sim 10\%$ ) in *both* films for a given power. The tunneling characteristic was then measured over this power range. The gap structure in the  $I$ - $V$  characteristic did not show any noticeable evidence of gap enhancement.

An unequivocal way to look for gap enhancement is by studying the second derivative signal from a tunnel junction. It has been shown earlier<sup>17</sup> that the phonon structure amplitude that appears in the second derivative of a tunnel junction is proportional to the square of the energy gap. Hence, if the gap is enhanced, one should be able to observe an increase in the amplitude of the phonon structure with microwave radiation. We feel that this is a very important experiment that should be performed, since the Al phonon structure appears at large voltages (17, 24 and 36 mV) compared to the energy gap and because this kind of a measurement is performed on the amplitude rather than the position of a structure in the  $I$ - $V$  characteristic.

#### 4. CONCLUSIONS

We have studied simultaneously the behavior of tunnel junctions and long superconducting bridges under microwave irradiation. We find that the classical rectification effect moves the structure in the tunnel junction  $I$ - $V$  characteristic in the same direction as expected from a gap enhancement. This classical effect is proportional to the square root of the microwave power. The classical effect can be simulated by superimposing a low-frequency (40 kHz) electric field on the junction. In the quantum limit, the effect of the radiation is to produce more and more microwave steps for increasing power.

We found that the critical currents of long bridges are more effectively enhanced by the magnetic microwave field rather than by the electric, although the dependence of the critical current enhancement on the microwave power is the same for both field configurations.

We do not understand why we are unable to measure any change in the tunneling curves that indicate gap enhancement, using samples and experimental techniques similar to those of Kommers and Clarke. We do observe microwave-enhanced critical currents, but the gap as measured by the tunnel junction remained unchanged.

## ACKNOWLEDGMENTS

We would like to thank Prof. John Clarke for useful conversations, and Drs. C. M. Falco, A. M. Goldman, K. E. Gray, P. E. Lindelof, and J. E. Mooij for helpful discussions. Our special thanks go to Prof. P. M. Chaikin, whose help, enthusiasm, and interest stimulated all of us.

## REFERENCES

1. T. M. Klapwijk and J. E. Mooij, *Physica* **81B**, 132 (1976); T. M. Klapwijk, J. W. van den Bergh, and J. E. Mooij, *J. Low Temp. Phys.* **2**, 385 (1977).
2. G. M. Eliashberg, *Zh. Eksp. Teor. Fiz. Pis. Red.* **11**, 186 (1970) [*Sov. Phys.—JETP Lett.* **11**, 114 (1970)].
3. Tom Kommers and John Clarke, *Phys. Rev. Lett.* **38**, 1091 (1977).
4. A. H. Dayem and P. J. Martin, *Phys. Rev. Lett.* **8**, 246 (1962).
5. Ivan Schuller, Thesis (1976), unpublished.
6. P. K. Tien and J. P. Gordon, *Phys. Rev.* **129**, 647 (1963).
7. C. A. Hamilton and Sidney Shapiro, *Phys. Rev. B* **2**, 4494 (1970).
8. James C. Swihart, *J. Appl. Phys.* **32**, 461 (1961).
9. V. A. Tulin, *Fiz. Nizk. Temp.* **2**, 1522 (1976) [*Sov. Phys.—J. Low Temp. Phys.* **2**, 741 (1976)].
10. P. W. Anderson and A. H. Dayem, *Phys. Rev. Lett.* **13**, 195 (1964).
11. A. H. Dayem and J. J. Wiegand, *Phys. Rev.* **155**, 419 (1967).
12. T. K. Hunt and J. E. Mercereau, *Phys. Rev. Lett.* **18**, 551 (1967).
13. P. E. Lindelof, *Sol. State Comm.* **18**, 283 (1976).
14. J. J. Chang and D. J. Scalapino, *Phys. Rev. B* **15**, 2651 (1977).
15. D. E. Dahlberg, to be published.
16. Ivan Schuller and K. E. Gray, *Phys. Rev. Lett.* **36**, 429 (1976); K. E. Gray and Ivan Schuller, *J. Low Temp. Phys.* **28**, 75 (1977).
17. P. M. Chaikin, G. Arnold, and P. K. Hansma, *J. Low Temp. Phys.* **26**, 229 (1977); B. F. Donovan-Vojtovic, Ivan Schuller, and P. M. Chaikin, to be published.